09SFL-0278

Robust Common-Rail Pressure Control for a Diesel-Dual-Fuel Engine Using QFT-Based Controller

Withit Chatlatanagulchai
Control of Robot and Vibration Laboratory (CRV Lab),
Department of Mechanical Engineering,
Faculty of Engineering, Kasetsart University, Thailand,
(E-Mail: fengwtc@ku.ac.th)

Tanet Aroonsrisopon
Department of Mechanical Engineering,
Faculty of Engineering, Kasetsart University, Thailand,
(E-Mail: fengtaa@ku.ac.th)

Krisada Wannatong
Energy Application Technique and Engine Lab Department,
PTT Research and Technology Institute,
PTT Public Company Limited, Thailand,
(E-Mail: krisada.w@pttplc.com)

ABSTRACT

Despite promising future, the diesel-dual-fuel engine, with diesel as pilot and natural gas as main, abounds with challenges from high NOx emission and knock especially at high speed and low load. To cope with these challenges, variation of common-rail pressure provides another desirable degree of freedom. Nevertheless, crippling with complicated dynamics, pressure wave inside the transporting rail, disturbance from varying of injections, engine speed variation, and actuator limitation, common-rail pressure control has relied on the simple PID to deliver only marginally satisfactory result. Some attempts to achieve better control have resulted in either too complicated or not too robust control system. We devise a controller from the quantitative feedback theory. Besides being able to quantitatively enforce specifications such as tracking, plant input and output disturbance rejections, and stability margin, the controller is designed from a simple model, whose parameters are allowed to be uncertain, hence robustness. The resulting controller has low order and is readily implementable. Experiment with a common-rail system in a Ricardo Hydra engine, modified to run dual fuel, shows the controller's effectiveness over the PID.

INTRODUCTION

In Thailand, there were about 300,000 diesel pickups sold each year. With minor modifications, instead of pure diesel, these diesel trucks can possibly use compressed natural gas as their main fuel to reduce total fuel cost.

This so-called diesel-dual-fuel engine needs to improve low-load characteristics, recognize and avoid knock at higher loads, and improve emission to fulfill legislative demands (especially HC and NOx emissions.) Even though engine parts need minor modifications, engine controller requires a total redesign to meet these challenges.

The Engineering Meetings Board has approved this paper for publication. It has successfully completed SAE's peer review process under the supervision of the session organizer. This process requires a minimum of three (3) reviews by industry experts.

ISSN 0148-7191

SAE Customer Service: Tel: 877-606-7323 (inside USA and Canada)
Tel: 724-776-4970 (outside USA)
Fax: 724-776-0790
Email: CustomerService@sae.org
SAE Web Address: http://www.sae.org

Printed in USA

SAE International

Varying common-rail pressure has been adopted as a possible means to improve engine performance. However, because the common-rail system has complicated dynamics and disturbances from adjacent systems such as the low-pressure pump and the injectors, a simple PID has generally been used since it does not require plant model. It is also well-known that the PID, although convenient, delivers merely satisfactory results.

In the past, researchers have proposed modeling and controls of the common-rail pressure that still leave some room for improvements.

Lino et al. [1] presented a control-oriented common-rail-system model, developed from physical laws. The model is simplified yet still nonlinear. The sliding-mode control is used for tracking. However, the signum function in the control law can cause excessive control shattering, and stability is not always guaranteed.

Coppo and Dongiovanni [2] developed a very detailed model for a common-rail system. The model was proved to match the experiment quite well. However, their model comprises some partial-differential equations, which are not appropriate for control design.

Balluchi et al. [3] proposed a hybrid model, with discrete and continuous interactions, of a common-rail system and showed that, with PID control, the proposed model delivered better tracking performance than the traditional mean-value model.

Morselli et al. [4] presented a common-rail system model based on energy principle. The model was shown to match an experiment quite closely. No attempt has been made to design controller.

Hu et al. [5] and Wu et al. [6] discussed pressure fluctuations and formulated a detailed model of the common-rail system. No attempt has been made to design controller.

It is evident that most work in the existing literature focus on detailed models to predict the common-rail system behavior. Very few contain control-oriented models. Publications that mention advanced control design, other than the simple PID, are almost non-existent.

In this paper, we first formed a model from actuated valve input signal to common-rail pressure. This model need not be very detailed nor accurate. We then applied a controller designed from the quantitative-feedback theory (QFT) to the closed-loop system. The controller is robust against model uncertainty and external disturbances, and the amount of robustness can be quantified. Simulation and experiment on a one-cylinder diesel-dual-fuel engine have shown better performance of the proposed controller over the traditional PID. Details on single-input-single-output (SISO) QFT is given in [7] whereas details on multi-input-multi-output (MIMO) QFT can be found in [8].

This paper is organized as follows. The next section contains brief description of the common-rail system, including details of our one-cylinder test bench. Then the section after that presents some QFT basics. System identification to find the model along with controller design are given in the subsequent section. We then present the experimental results and closed with conclusions.

COMMON-RAIL INJECTION SYSTEM

Figure 1 depicts a general common-rail injection system. A high-pressure pump receives fuel from a low-pressure pump, which connects to the fuel tank (not shown in Figure 1.) Inside the high-pressure pump, a metering unit functions as a gate to allow more or less fuel to the common rail. By varying the duty cycle, a PWM signal is sent from the ECU to a solenoid to control the lift of a plunger gate inside the metering unit (In some engine models, however, there is another regulator valve inside the common rail.) A pressure sensor is used to measure pressure inside the rail whereas a relief valve returns the fuel to the fuel tank. The ECU also actuates each diesel injector in each cylinder.

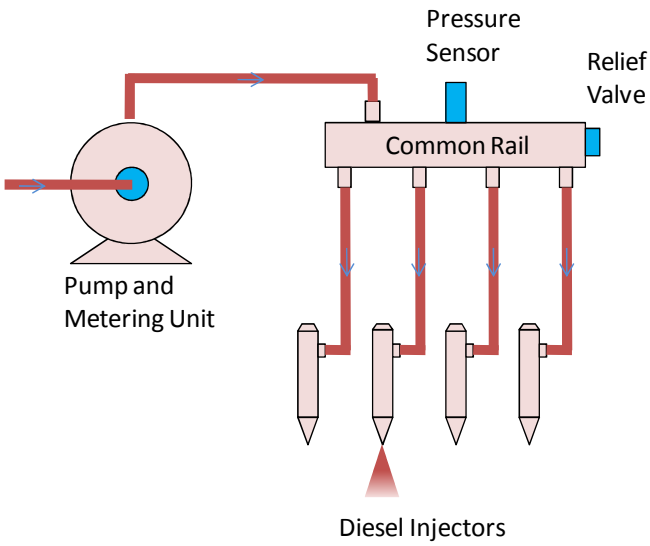

Figure 1: Schematic of a common-rail diesel-injection system.

We experimented on the common-rail system of a single-cylinder, two-valve, and four-stroke Ricardo Hydra engine. This engine was modified to run diesel-dual-fuel. Table 1 lists specifications of this engine.

Table 1: 2-Valve DI Diesel Ricardo Hydra Engine Specifications.

Number of cylinders:	1 cylinder
Number of valves:	2 valves
Combustion chamber:	Direct Injection
Fuel system:	Common rail
Displacement volume:	449.77 cc
Bore:	80.26 mm
Stroke:	88.90 mm
Connecting rod:	158.0 mm
Compression ratio:	20.36:1 (Calculated)
Aspiration:	Normally Aspirated
Rated speed:	4,500 rpm
Maximum speed:	4,500 rpm
Coolant outlet temperature:	85°C
Oil inlet temperature:	85°C
Tappet clearance (cold):	0.3 to 0.4 mm
Valve timings: IVO IVC EVO EVC	 8° before TDC (+352° after firing TDC) 42° after BDC (–138° after firing TDC) 60° before BDC (+120° after firing TDC) 12° after TDC (–348° after firing TDC)

QFT BASICS

QFT (quantitative feedback theory) was developed almost sixty years ago by I. Horowitz [9]. It is a frequency-based design technique that extends the work of H. W. Bode [10] to a more quantitative way, resulting in a robust frequency-domain controller. Although QFT was originated decades ago, its applications have just been accelerated in the late 80's and early 90's due to the advent of the QFT computer-aided-design (CAD) packages [11]-[13].

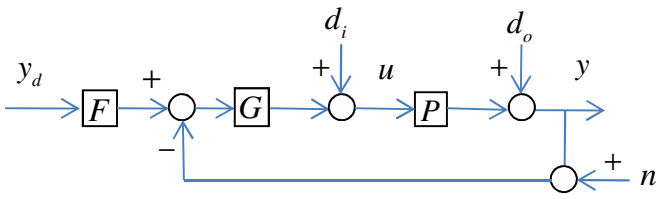

Figure 2: A two-degrees-of-freedom closed-loop system.

Block diagram of a two-degree-of-freedom closed-loop system is given in Figure 2. We would like to have the common-rail pressure track an arbitrary reference closely, so y is the common-rail pressure and y_d is the reference.

The plant P maps the duty cycle of the PWM signal sending to the solenoid of the metering unit, u, to the common-rail pressure from the rail's pressure sensor, y.

The tracking must be good under the presence of model uncertainty; pressure sensor noise; variations of the injector dynamics, engine speed, and fuel temperature; reversal flow; pressure wave inside the connecting rail; and variation of the metering-unit dynamic.

Instead of on a single nominal plant P, a controller G and a prefilter F will be designed on $\{P\}$, a set containing several variations of P. This takes model uncertainty into account since the controller design phase, ensuring robustness of the closed-loop system.

In Figure 2, pressure sensor noise can be viewed as the measurement noise n whereas variation of the metering-unit dynamic can be viewed as the plant-input disturbance d_i and all the other variations can be viewed as the plant-output disturbance d_o.

QFT-based design process has three steps, which are developing frequency-domain specifications, generating bounds, and performing loop shaping.

Specifications may be given in time or frequency domain. If it is given in the time domain, it must be converted to the frequency domain. Specifications are tracking, disturbance rejection, noise rejection, stability margin, and control effort. For example, in tracking, we would want $\left|FGP/(1+GP)\right|$ to be close to one. In plant-output disturbance rejection, we would want $\left|1/(1+GP)\right|$ to be less than a small number.

From the frequency-domain specifications, bounds are generated on the Nichols chart, a chart having Bode gain as its vertical axis and Bode phase as its horizontal axis. For a specific frequency, the plant set $\{P\}$, called plant template, appears as a group of points on the Nichols chart. All points must be included when generating a bound to involve all plant uncertainties. The worst-case bounds are the strictest bounds among all specifications at a frequency. There is only one worst-case bound per frequency.

On the Nichols chart, the loop shaping involves shaping of the controller G and the prefilter F so that the resulting open-loop shape satisfies all bounds at all frequencies.

In summary, a QFT-based controller is robust against plant uncertainty since it is designed from the plant

template. The controller is also robust against external disturbances and noise since they are specified in the specifications. The tracking performance and control effort can also be specified. This robustness property makes it a good controller to be used in common-rail pressure control.

CONTROL DESIGN

To find the nominal plant P, the input's duty cycle u is altered as a frequency-varying sine wave, spanning over a range of frequencies. The resulting output rail pressure y is noted, and the input-output signals are used in the Matlab's identification toolbox to obtain a second-order linear model

$$\frac{Y}{U} = \frac{5.0725}{4.7721s^2 + 0.5098s + 1},$$

where Y and U are the Laplace transformations of y and u. The model above was validated, and the result is given in Figure 3, where the dotted line is the actual pressure y, and the solid line is the model output y_m. The nominal plant is shown to be an acceptable imitation of the actual common-rail system.

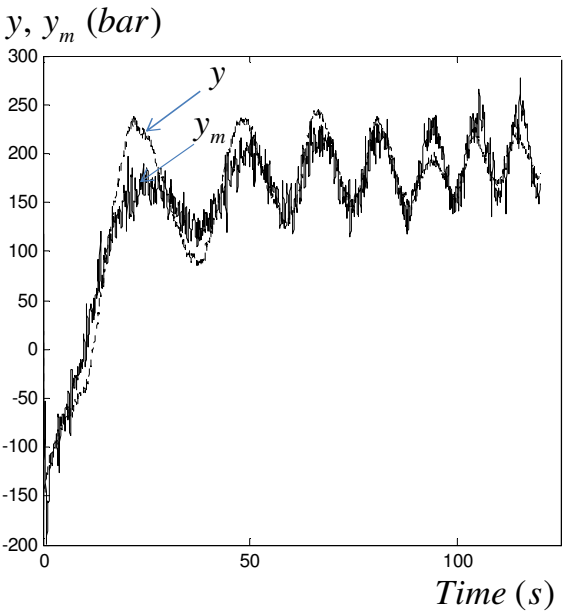

Figure 3: Validation result of the nominal plant model.

We add 30% parameter variations to each parameter in our simplified nominal plant P. For a specific frequency, on the Nichols chart, instead of a single point, we have a group of points, each point marks a single plant having a specific set of parameter values. As mentioned previously, these groups of points are called plant templates. The controller will be designed on these plant templates to ensure that the resulting closed-loop system will meet our design specifications for up to 30% parameter variations. Figure 4 shows the plant templates for frequencies 0.01, 0.1, 0.5, 1, and 2 rad/s. The stars locate the nominal plants.

For tracking specification, we let

$$|\beta| < |FGP/(1+GP)| < |\alpha|, \quad (1)$$

where α and β are the transfer functions $0.2625/(s^2+s+0.25)$ and $0.0855/(s^2+0.6s+0.09)$, respectively. Notice that they are second-order transfer functions with appropriate parameter values to produce desirable shapes of the upper and lower bounds in time domain.

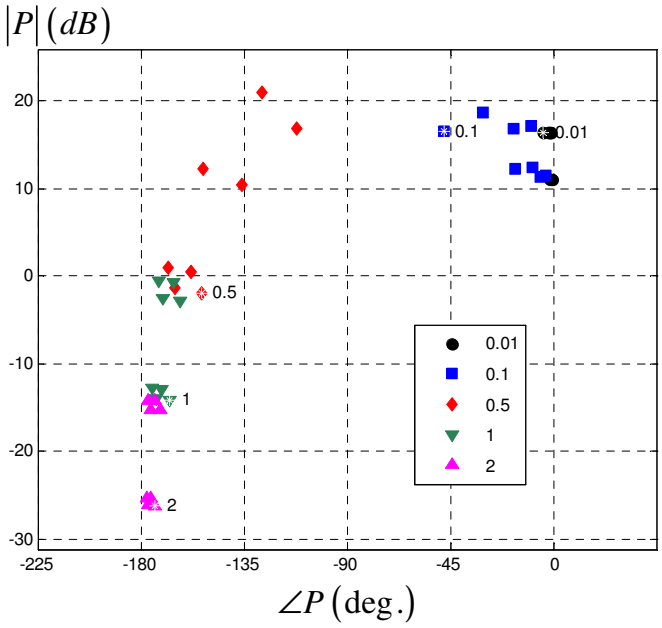

Figure 4: Plant templates on the Nichols chart at various frequencies.

From the Nyquist criterion, it can be shown that the stability margin specification can be given in the form

$$|1/(1+GP)| < \delta, \quad (2)$$

which is identical to the plant output disturbance rejection specification. We choose $\delta = 4\,dB$.

After the templates and the frequency-domain specifications are obtained, creating bounds on the Nichols chart can be done, for a frequency ω, by fixing a phase ϕ and determining a boundary point, marked by the nominal plant, where the specification is met for all plants in the template. A line is then obtained from varying the phase to cover the whole 360°. Details of bounds creation can be found in the QFT textbook [14]. Figure 5 shows tracking and stability (or plant output disturbance rejection) bounds. For various frequencies, the solid lines mark the tracking bounds, and the dotted lines mark the stability bounds.

In the complex plane, specifications (1) and (2) require that $L = GP$ must lie outside of an area enclosing the point $(-1, 0)$. On the Nichols chart, this valid region corresponds to the area above or outside of the bound. The controller G can then be designed such that the open-loop L lies on the valid region for all frequencies under consideration.

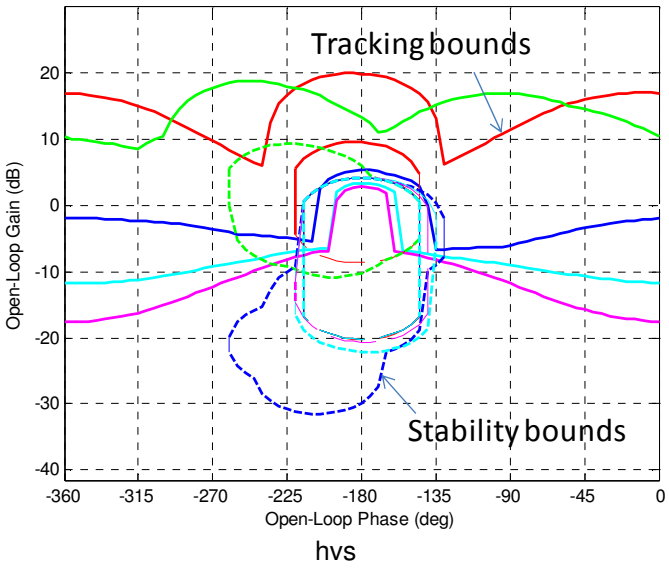

Figure 5: Tracking and stability bounds.

By appending a lead in the form $(s/z+1)/(s/p+1)$ and a real pole in the form $1/(s/p+1)$ to an appropriate gain, we get an open-loop shape as a solid line in Figure 6.

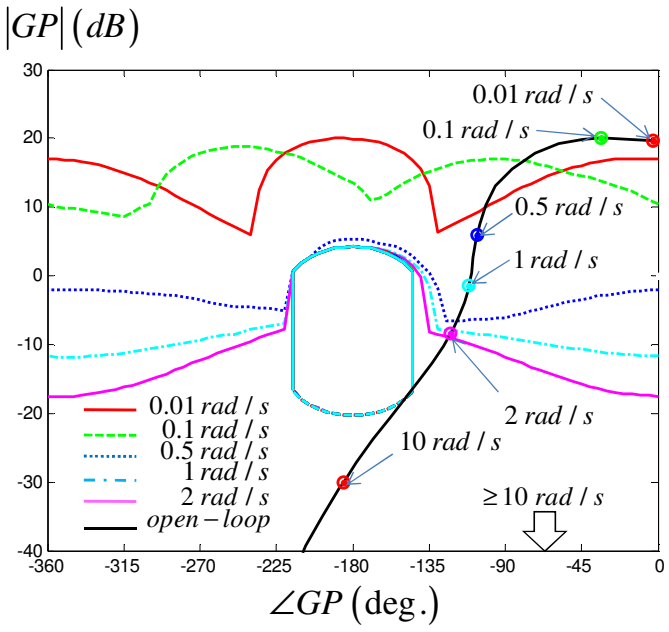

Figure 6: Open-loop shape and worst-case bounds.

With a sampling period of $20\,ms$, the controller G in discrete time is given by

$$G(z) = \frac{5.469z - 5.43}{z^2 - 1.63z + 0.6562},$$

where z is the z-transform operator.

Whereas the controller G is designed to reduce the variation of $|FGP/(1+GP)|$ to be narrower than the tracking specification (1), the prefilter F is needed to shift the closed-loop Bode plots so that they are within the specification boundaries.

The prefilter F contains two real poles and is given in discrete time by

$$F(z) = \frac{4.32\times10^{-5}z + 4.287\times10^{-5}}{z^2 - 1.977z + 0.9775}.$$

Figure 7 shows the result of including the prefilter in the closed-loop system. The dotted lines are upper and lower bounds whereas the solid lines are the closed-loop magnitudes for all possible plant variations.

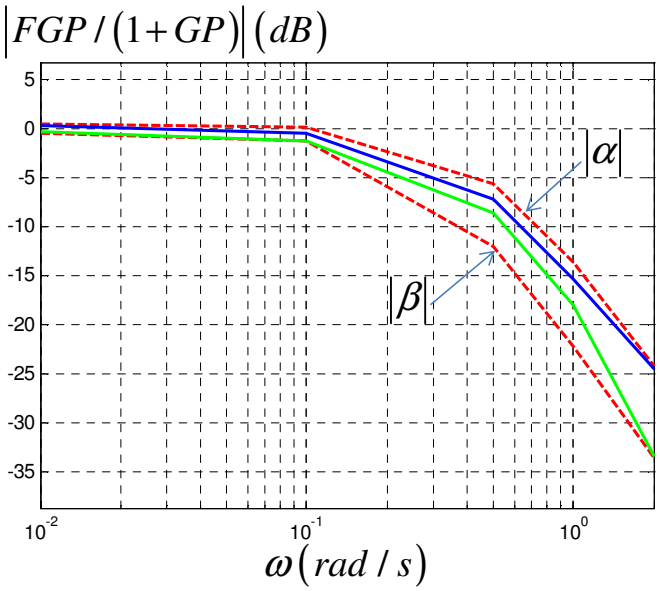

Figure 7: Closed-loop magnitude with upper and lower bounds.

Figure 8 shows tracking performance in time domain. UB is obtained by passing a square wave into the upper-bound transfer function α, and LB is obtained by passing the same square wave into the lower-bound transfer function β. We may tighten the tracking specification by adjusting parameters in α and β. For all plant variations, the closed-loop output pressure y is able to follow the desired value closely and within the pre-specified upper and lower bounds.

The plant output disturbance rejection performance is measured by the ability of the closed-loop system to

attenuate the effect of the disturbance to the output. To see this, we let the plant-output disturbance d_o be a square wave with 300 in magnitude. The output y as a result of this disturbance is shown in Figure 9 where good attenuation result can be seen.

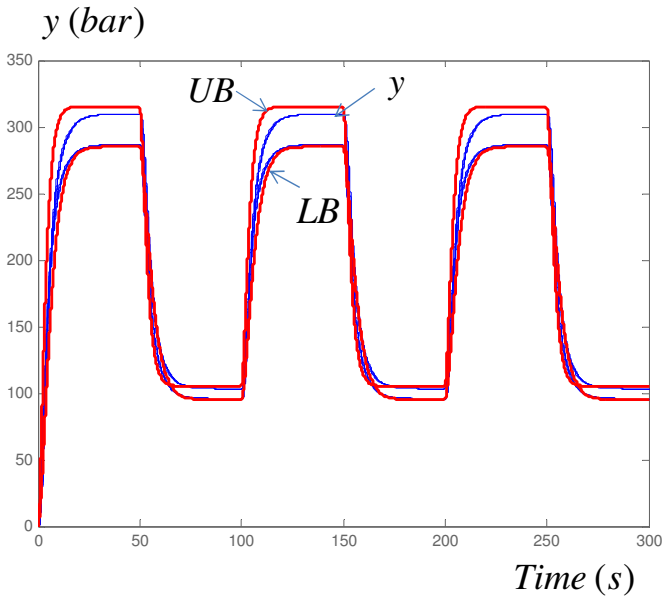

Figure 8: Simulation result: tracking performance in time domain.

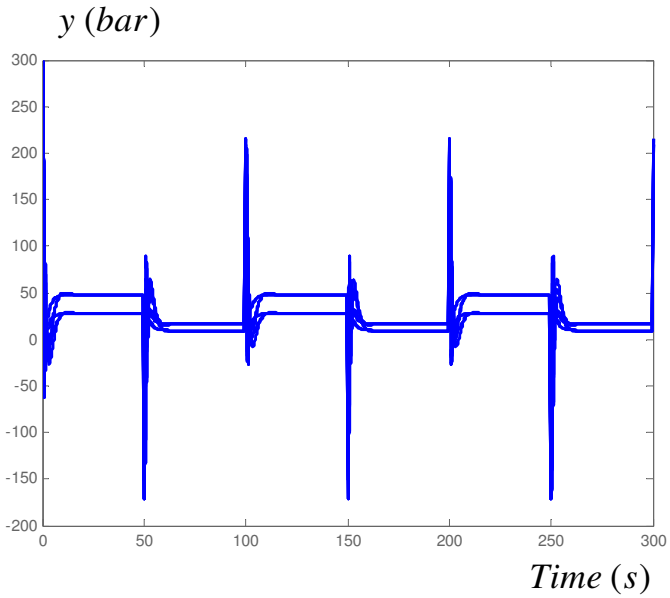

Figure 9: Simulation result: plant output disturbance rejection in time domain.

Figure 10 and Figure 11 show performance in frequency domain. In Figure 10, the closed-loop magnitudes for all plant variations fall within the bounds until $2\ rad/s$. This is because we only include frequencies upto $2\ rad/s$ in our design to avoid having too high gain over high frequency range, which may amplify high-frequency noise.

The stars in Figure 11 mark the $4\,dB$ specification. It can be seen that the specification is met for all plant variations for all designed frequencies.

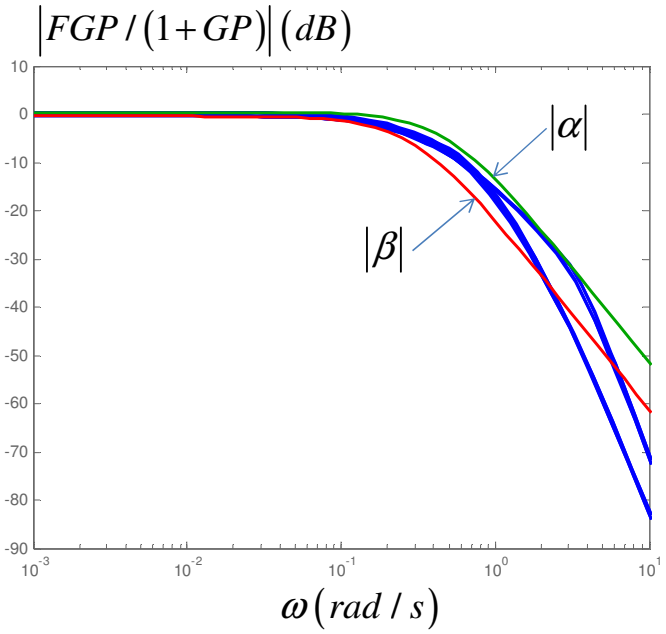

Figure 10: Simulation result: tracking performance in frequency domain.

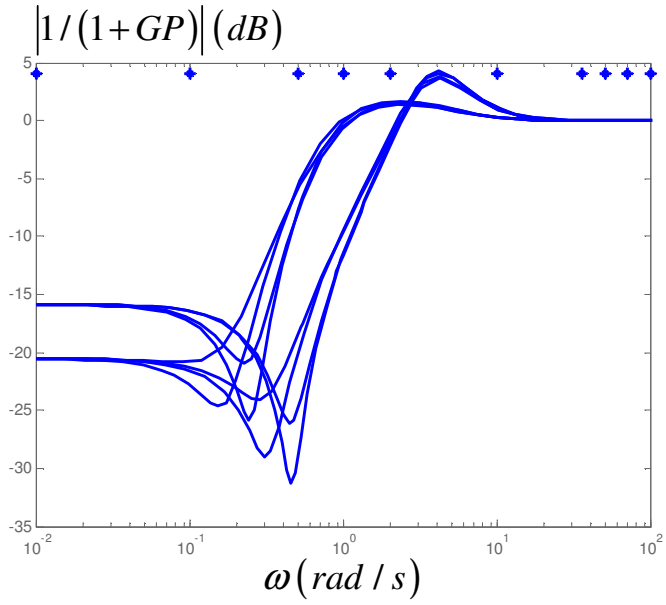

Figure 11: Simulation result: plant output disturbance rejection in frequency domain.

EXPERIMENTAL RESULTS

The controller and the prefilter in the previous section are applied to the test bench. The details of the test bench are given in Table 1.

We compare our proposed controller and prefilter with the PID control, where best attempt is spent to adjust the PID gains to obtain best tracking result possible.

In part (a) of Figure 12 and Figure 13, the dotted lines represent operator-given desired common-rail pressure whereas the solid lines represent the actual common-rail pressure. In part (b), the duty cycle percentage input to the solenoid of the pump's metering unit is shown.

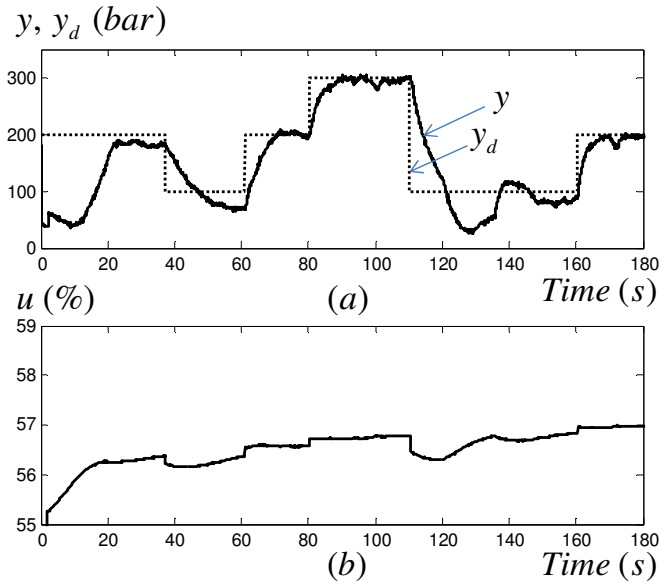

Figure 12: Experimental result using a PID controller. a) Output pressure versus its desired value. b) Control input as duty cycle percentage.

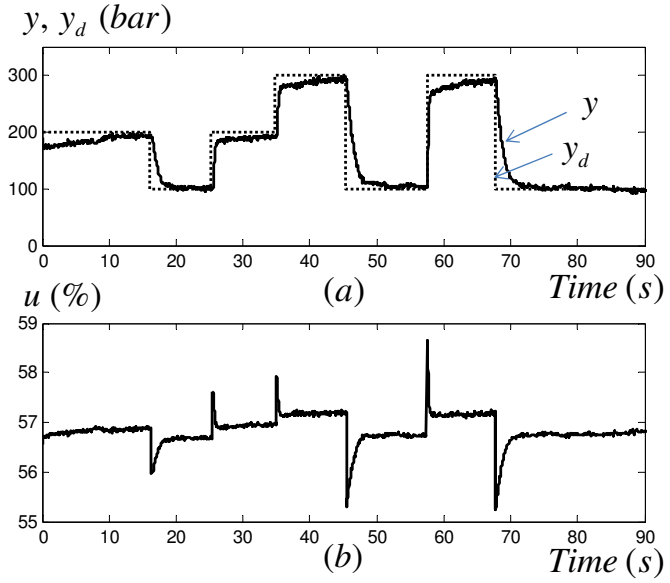

Figure 13: Experimental result using the QFT-based controller. a) Output pressure versus its desired value. b) Control input as duty cycle percentage.

Under the same test bench condition, it can be seen from the results that the proposed QFT-based control delivers significantly better performance than that of the PID. Note also the time scale difference in the plots of both figures. The QFT-based control achieves faster settling time and less steady-state error.

CONCLUSIONS

For a complicated process such as the common-rail system, the QFT-based controller achieves better tracking performance than the traditional PID controller. The performance can be quantitatively specified in terms of tracking, stability, and disturbance rejection specifications.

The test bench has only one cylinder, so we cannot evaluate the effect of cylinder interaction. But there is high possibility that the QFT-based controller will still deliver better performance.

The QFT-based controller is simple and robust, hence suitable for other engine control applications such as the EGR or the injector controls, which are where future research efforts might be spent.

ACKNOWLEDGMENTS

We thank Craig Borghesani and Terasoft, Inc for their evaluation copy of the QFT toolbox. This work was conducted at and funded by the PTT Research and Technology Institute, PTT Public Company Limited, Thailand.

REFERENCES

[1] P. Lino, B. Maione, and A Rizzo, "Nonlinear modeling and control oa a common rail injection system for diesel engines," *Applied Mathematical Modelling*, Vol. 31, 1959, pp. 1770-1784.

[2] M. Coppo and C. Dongiovanni, "Experimental validation of a common-rail injector model in the whole operation field," *Journal of Engineering for Gas Turbines and Power*, Vol. 129, 2007, pp. 596-608.

[3] A. Balluchi, A. Bicchi, E. Mazzi, A. S. Vincentelli, and G. Serra, "Hybrid modeling and control of the common rail injection system," *Int. Journal of Control,* Vol. 80, No. 11, 2007, pp. 1780-1795.

[4] R. Morselli, E. Corti, and G. Rizzoni, "Energy based model of a common rail injector," *Proc. of the 2002 IEEE Int. Conf. on Control App,* Glasgow, Scotland, September 2002, pp. 1195-1200.

[5] Q. Hu, S. F. Wu, S. Stottler, and R. Raghupathi, "Modelling of dynamic responses of an automotive fuel rail system, part I: injector," *Journal of Sound and Vibration,* Vol. 245, No. 5, 2001, pp. 801-814.

[6] S. F. Wu, Q. Hu, S. Stottler, and R. Raghupathi, "Modelling of dynamic responses of an automotive

fuel rail system, part II: injector," *Journal of Sound and Vibration,* Vol. 245, No. 5, 2001, pp. 815-834.
[7] W. Chatlatanagulchai, B. Inseemeesak, and W. Siwakosit, "Quantitative feedback control of a pendulum with uncertain payload," *Journal of Research in Engineering and Technology*, Vol. 4, No. 4, October 2007, pp. 347-367.
[8] W. Chatlatanagulchai, C. Srinangyam, and W. Siwakosit, "Trajectory control of a two-link robot manipulator carrying uncertain payload using quantitative feedback theory," *Journal of Research in Engineering and Technology*, Vol. 5, No. 1, Jan 2008, pp. 45-71.
[9] I. Horowitz, "Fundamental theory of linear feedback control systems," *Trans. IRE on Auto. Control*, AC-4, Dec. 5-19, 1959.
[10] H. W. Bode, *Network Analysis and Feedback Amplifier Design*, Van Nostrand, 1945.
[11] C. Borghesani, *Computer Aided-Design of Robust Control Systems Using the Quantitative Feedback Theory*, M.S. Thesis, Mechanical Engineering Department, University of Massachusetts, Amherst, MA, 1993.
[12] R. R. Sating, *Development of an Analog MIMO Quantitative Feedback Theory (QFT) CAD Package*, M.S. Thesis, Graduate School of Engineering, Air Force Institute of Technology, Wright Patterson AFB, OH, 1992.
[13] C. H. Houpis and G. Lamont, *Digital Control Systems: Theory, Hardware, Software*, McGraw-Hill, NY, 2nd Ed., 1992.
[14] I. Horowitz, *Quantitative Feedback Design Theory – QFT,* QFT Publications, CO, USA, 1993.

CONTACT

Withit Chatlatanagulchai received MS and PhD degrees in mechanical engineering (systems, dynamics, and control) from Purdue University, USA in 2006. His research interests are engine and vibration controls using advanced algorithms such as nonlinear control, intelligent systems, QFT, H_2 and H_∞ control, adaptive control, and command input shaping method. For more information, the readers may browse http://www.crvlab.eng.ku.ac.th/.